

# Generating Property-Directed Potential Invariants By Backward Analysis

Adrien Champion

Onera, The French Aerospace Lab  
Toulouse, France

Rockwell Collins France  
Blagnac, France

adrien.champion@onera.fr

Rémi Delmas

Onera, The French Aerospace Lab  
Toulouse, France

remi.delmas@onera.fr

Michael Dierkes

Rockwell Collins France  
Blagnac, France

mdierkes@rockwellcollins.com

This paper addresses the issue of lemma generation in a  $k$ -induction-based formal analysis of transition systems, in the linear real/integer arithmetic fragment. A backward analysis, powered by quantifier elimination, is used to output preimages of the negation of the proof objective, viewed as unauthorized states, or *gray states*. Two heuristics are proposed to take advantage of this source of information. First, a thorough exploration of the possible partitionings of the gray state space discovers new relations between state variables, representing potential invariants. Second, an inexact exploration regroups and over-approximates disjoint areas of the gray state space, also to discover new relations between state variables.  $k$ -induction is used to isolate the invariants and check if they strengthen the proof objective. These heuristics can be used on the first preimage of the backward exploration, and each time a new one is output, refining the information on the gray states. In our context of critical avionics embedded systems, we show that our approach is able to outperform other academic or commercial tools on examples of interest in our application field. The method is introduced and motivated through two main examples, one of which was provided by Rockwell Collins, in a collaborative formal verification framework.

## 1 Introduction

The recent DO-178C and its formal methods supplement DO-333 published by RTCA<sup>1</sup> acknowledge the use of formal methods for the verification and validation of safety critical flight control software and allow their use in development processes. Successful examples of industrial scale formal methods applications exist, such as the verification by Astrée [4] of the run-time safety of the Airbus A380 flight control software C code. However, the verification of general functional properties at model level, *i.e.* on Lustre [7] or MATLAB Simulink© programs, from which the embedded code is generated, still requires expert human intervention to succeed on common avionics software design patterns, preventing industrial designers from using formal verification on a larger scale. Formal verification at model level is important, since it helps raising the confidence in the correctness of the design at early stages of the development process. Also, the formal properties and lemmas discovered at model level can be forwarded to the generated code, in order to facilitate the final design verification and its acceptance by certification authorities [12]. Our work addresses some of the issues encountered when attempting formal verification of properties of synchronous data flow models written in Lustre. We propose a property-directed lemma generation approach, together with a prototype implementation. The proposed approach aims at reducing the amount of human intervention usually needed to achieve  $k$ -induction proofs, possibly using *abstract*

---

<sup>1</sup><http://www.rtca.org/>

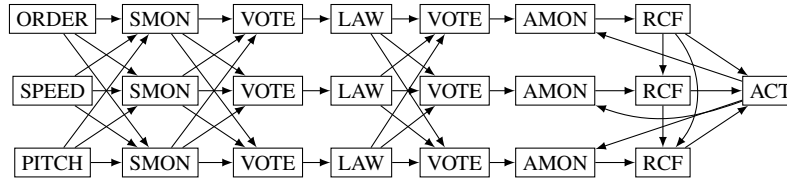


Figure 1: Shuffled, triple channel architecture

*interpretation* technique in cooperation. Briefly outlined, the approach consists first in an abstract interpretation pass to discover coarse bounds on the numerical state variables of the system; a  $k$ -induction engine and our lemma generation techniques are then ran in parallel to search for potential invariants in order to strengthen the property. We insist on the fact that the primary goal of the proposed method is discovering missing information needed to prove properties the verification of which is either very expensive or impossible with currently available methods and tools, rather than improving the performance of the verification of properties which are already relatively easily provable.

The paper is structured as follows: Section 2 describes the embedded software architectures targeted by our work. Related work and tools are discussed in Section 3 before notations and vocabulary are given in Section 4. A description of the underlying  $k$ -induction engine assumed in this paper follows in Section 5. We introduce and motivate our approach in Section 6 and detail the lemma generation techniques in Section 7. The proposed approach is then illustrated on a reconfiguration logic example and on Rockwell Collins industrial triplex sensor voter in Section 8. Implementation is briefly discussed in Section 9, before concluding in Section 10.

## 2 Fault Tolerant Avionics Architectures

We consider embedded reactive software functions which contribute to the safe operation of assemblies of hardware sensors, networked computers, actuators, moving surfaces, *etc.* called *functional chains*. A functional chain can for instance be in charge of "controlling the aircraft pitch angle", and must meet both qualitative and quantitative safety requirements depending on the effects of its failure. Effects are ranked from MIN (minor effect) to CAT (catastrophic effect, with casualties). For instance, the failure of a pitch control function is ranked CAT, and the function shall be robust to at least a double failure and have an average failure rate of at most  $10^{-9}$  per flight hour. In order to meet these requirements, engineers must introduce hardware and software redundancy and implement several fault detection and reconfiguration mechanisms in software.

A frequently encountered architectural design pattern, triplication with shuffle, is depicted in Fig. 1. It allows to recover from single failures and to detect double failures. Data sources, data processing hardware and functions are triplicated to obtain three *channels*. The actuator is not replicated. Data is locally monitored right after acquisition/production, but is also broadcast across channels to be checked using triplex voting functions, in order to detect complex error situations. Last, in each channel, depending on the fault state of the channel and the observable behavior of other channels, the *reconfiguration logic* decides whether the channel in question must take control of the actuator or on the contrary mute itself. Being *healthy* for a channel means that no fault has occurred for a sufficient amount of consecutive time steps to become *confirmed*.

Previous work by our team addresses the formal verification of control laws numerical stability [24], yet ensuring proper behavior of *voting functions* and *reconfiguration logic* as introduced here is equally important, for these building blocks and design patterns are ubiquitous in fault tolerant avionics soft-

ware. For the voting logic, we focus on BIBO properties, “bounded input implies bounded output”, the verification of which is detailed in Section 8.2. For reconfiguration logic, which makes an extensive use of integer timers and discrete logic, we focus on bounded liveness properties such as “assuming at most two sensor, network or CPU faults, the actuator must never remain idle for more than  $N$  consecutive time units”, the verification of which is addressed in Section 8.1.

### 3 Related Work and Tools

In this section we review the state of the art of verification tools relevant in our application domain, *i.e.*, of currently available tools and techniques allowing to address synchronous data flow models written in Lustre. We distinguish two main families of verification approaches.

First, approaches based on abstract interpretation (AI [9]). The tool NBac [15] for instance allows to analyze properties of Lustre models by using a combination of forward and backward fixpoint computation using AI. AI tends to need expert tuning for the choice of abstract domains, partitioning, *etc.* to behave correctly on the systems we consider. NBac proposes a heuristic selection of AI parameter tuning, which dynamically refines domains and partitionings to try to obtain a better precision without falling in a combinatorial blowup.

Second, the family of  $k$ -induction [25] based approaches, with the commercial tool Scade Design Verifier<sup>2</sup>, or the academic tool Kind [17]. Kind is the most recently introduced tool, and wraps the  $k$ -induction core in an automatic counter example guided abstraction refinement loop whereas the Scade Design Verifier does not.  $k$ -induction is an exact technique, in which little or no abstraction is performed (the concrete semantics of the program is analyzed). Experiments show that it does not scale up out of the box on the systems encountered in our application field. Proving proof obligations on such systems often requires to unroll the system’s transition relation to the reoccurrence diameter of the model which can be very large in practice (hundred or thousands of transitions). For such proof obligations, which are either  $k$ -inductive for a  $k$  too large to be reached in practice, or even non-inductive at all, numerical lemmas are needed to help better characterize the reachable state space and facilitate the inductive step of the reasoning.

In order to address this common issue with  $k$ -induction, automatic lemma generation techniques have been studied. Two main approaches can be distinguished. First, property agnostic approaches, such as [16], in which template formulas are instantiated in a brute force manner on combinations of the system state variables to obtain a set of potential invariants. They are then analyzed alongside the PO using the main  $k$ -induction engine. Second, property directed approaches, such as [6, 5], in which the negation of root states of counterexamples are used as strengthening lemmas, with or without generalization, or are used to guide template instantiation. Also worth mentioning, interpolation [18] yields very interesting results in lemma generation but unfortunately to our knowledge no interpolation tool analyzing Lustre code exists.

We consider a lemma generation pass successful when the generated potential invariants allow to prove the original proof objective with a  $k$ -induction run with a small  $k$ . Once the right lemmas are found, the proof can be easily re-run and checked by third party  $k$ -induction tools, an important criterion for industrials and certification organisms. As we will see in the rest of the paper, the lemma generation approach proposed in this paper takes inspiration from all the aforementioned techniques : while somehow brute force in its exploration of the gray state space partitionings, our approach discovers relevant lemmas thanks to its property-directed nature.

---

<sup>2</sup><http://www.esterel-technologies.com/products/scade-suite/add-on-modules/design-verifier>

## 4 Notations

Let us now define several notions used throughout this paper. First, a *transition system* is represented as a tuple  $\langle v, D, I(v), T(v, v') \rangle$  where  $v$  is a vector of state variables,  $D$  specifies the domain of each state variable, either boolean, integer or real valued,  $I$  is the initial state predicate, and  $T$  is the transition predicate in which  $v'$  represents next state variables. The logic used to express predicates is Linear Integer or Real Arithmetic with Booleans. The usual notions of trace semantics and reachability are used. Given a formula  $PO(v)$  representing a Proof Objective (PO), we say that the PO holds if no state  $s$  such that  $\neg PO(s)$  can be reached from  $I$  through repeated application of  $T$ . Lustre or Scade programs can be cast into this representation using adequate compilers.

An *atom* is a Boolean or its negation, or a linear equality or inequality in LRA or LIA. A *polyhedron* is a conjunction of atoms. More precisely, we will say polyhedron for not necessarily closed polyhedron, meaning that we do not impose restrictions on the form of the inequalities besides linearity. The *convex hull* of two polyhedra  $p_1$  and  $p_2$  is the smallest polyhedron such that it contains  $p_1$  and  $p_2$ . We will say that the convex hull  $h$  of two polyhedra  $p_1$  and  $p_2$  is *exact* if and only if  $h = p_1 \cup p_2$ , and call it the *Exact Convex Hull* (or ECH) of  $p_1$  and  $p_2$  if it exists. For the sake of clarity, convex hulls that are not necessarily exact will be called *Inexact Convex Hulls* (or ICH). Note that for integer variables, the uniqueness of the convex hull is not guaranteed if non-integer values for the coefficients are not forbidden. We ban them in the rest of this paper; in our implementation, it is prevented by the type system. Still, there are several ways to represent the same inequality, e.g.  $n > 0$  and  $n \geq 1$ . Despite their difference in representation, these polyhedra enclose the same (integer) points geometrically speaking, so this does not hinder our approach. Convex hull comparison in this paper does not rely on their syntax nor semantics, but rather on the *source* of the hull, i.e. the original polyhedra used to create them. This will be discussed in Section 7 during the explanation of our main contribution, the *hullification* algorithm.

## 5 Proofs by Temporal Induction

The Stuff framework provides an SMT-based  $k$ -induction module. Performing a  $k$ -induction analysis of a potential state invariant  $P$  on a transition system  $\langle I, T \rangle$  consists in checking the satisfiability of the  $Base_k(I, T, P)$  and  $Step_k(T, P)$  formulas, defined in (1), for increasing values of  $k$ , starting from a user specified  $k > 1$ .

$$\begin{aligned}
 Base_k(I, T, P) &\equiv \overbrace{I(s_0)}^{\text{Initial state}} \wedge \underbrace{\bigwedge_{i \in [0, k-2]} T(s_i, s_{i+1})}_{\text{trace of } k-1 \text{ transitions}} \wedge \underbrace{\bigvee_{i \in [0, k-1]} \neg P(s_i)}_{P \text{ falsified on some state}} \\
 Step_k(T, P) &\equiv \underbrace{\bigwedge_{i \in [0, k-1]} T(s_i, s_{i+1})}_{\text{trace of } k \text{ transitions}} \wedge \underbrace{\bigwedge_{i \in [0, k-1]} P(s_i)}_{P \text{ satisfied on first } k \text{ states}} \wedge \underbrace{\neg P(s_k)}_{P \text{ falsified by last state}}
 \end{aligned} \tag{1}$$

The base and step instances are analysed, until either a base model has been found, in which case the proof objective is falsified, a user specified upper bound for  $k$  has been reached for base and step, in which case the status of the proof objective is still undefined, or a  $k$  value has been discovered so that both formulas are unsatisfiable, which proves the validity of the objective.

In addition, this  $k$ -induction engine allows, for any  $n$ , to partition a given set of proof objectives  $P = \{P_j\}$ , viewed as a conjunction  $P = \bigwedge_j P_j$ , in three maximal subsets  $F_n$ ,  $U_n$  and  $V_n$ , such that:

- elements  $P \in F_n$  are such that  $Base_n(I, T, P)$  is satisfiable: they are *Falsified*;
- elements  $P \in U_n$  are such that  $Base_n(I, T, P)$  is unsatisfiable and  $Step_n(T, P)$  is satisfiable: they are *Undefined* because neither falsifiable nor  $n$ -inductive;
- elements of  $V_n$  are such that  $Base_n(I, T, \bigwedge_{P \in V_n} P)$  is unsatisfiable and  $Step_n(T, \bigwedge_{P \in V_n} P)$  is unsatisfiable: they are mutually  $n$ -inductive, *i.e.* *Valid* on the transition system.

## 6 Approach Overview: Backward Exploration and Hull Computation

Our lemma generation heuristic builds on a backward property-directed reachability analysis. We use Quantifier Elimination (QE [19, 22, 3]) to compute successive preimages of the negation of the PO, in the spirit of [21, 10]. In our approach, the states characterized by the preimages are generated in a way such that (i) they satisfy the PO and (ii) from them, it is possible to reach a state violating the PO if certain transitions are taken. Such states will be referred to as *gray states*. This can be achieved by calculating the preimages as follows:

$$\begin{aligned} preimage_1 &= QE(s', PO(s) \wedge T(s, s') \wedge \neg PO(s')) \\ preimage_i &= QE(s', PO(s) \wedge T(s, s') \wedge preimage_{i-1}[s'/s]) \quad (\text{for } i > 1) \end{aligned} \quad (2)$$

where  $QE(\vec{v}, F)$  returns a quantifier-free formula equisatisfiable to  $\exists \vec{v}, F$  and such that  $FV(QE(\vec{v}, F)) = FV(F) \setminus \vec{v}$ . The preimages themselves are assumed to be in DNF, by using [19] as a QE engine for instance.

From these preimages we extract information using two search heuristics introduced and motivated in the rest of this section and detailed in Section 7. These heuristics run in parallel, alongside the backward analysis computing the next preimage and a  $k$ -induction engine. The backward analysis is not run to a fixed point before proceeding further, it is rather meant to probe the gray state space around the negation of the PO, and feeding the potential lemma generation with the preimages as soon as they are produced.

To extract information out of the preimages, at any point of the backward exploration, their disjunction is considered: it represents the gray states found so far as a union of polyhedra. The main idea underlying the potential lemma generation is to explore the ways in which those polyhedra can be grouped using convex hull calculation, thus discovering linear relations over state variables representing boundaries between convex regions of the gray state space. Since these convex boundaries enclose unauthorized states, they are negated before being sent to our  $k$ -induction engine to check their validity and try to strengthen the PO.

The PO is successfully strengthened by a set of lemmas when the set  $V_k$  of valid POs, produced by the  $k$ -induction analysis detailed in Section 5, contains the main PO at the end of a run. If the original PO is not strengthened by the potential invariants extracted from the currently available preimages, a new preimage is calculated, bringing more information. Yet, when the PO is strengthened and proved valid, it can be the case that not all elements of the valid subset  $V_k$  are needed to entail the original PO. A minimization pass inspects them one by one, discarding  $l \neq PO$  from  $V_k$  if  $\bigwedge(V \setminus l)$  remains  $k$ -inductive, to obtain a relatively small and readable set of lemmas.

Note that, in the backward exploration, the choice of which variables to eliminate by QE and which to keep is important. Eliminating the next state variables and keeping the current state variables is not satisfactory in the general case, as on large scale systems, many state variables might not be relevant for the PO under investigation, and might hinder the performance of the convex hull calculation or  $k$ -induction. Therefore, the only state variables that are **not** eliminated are the ones found in the cone of

influence of the PO, in their *current state* version. In particular, the system inputs are eliminated since they do not provide more information from a backward analysis point of view.

Before going into the details of the potential lemma generation algorithm, let us illustrate how computing ICHs and ECHs can actually make new numerical relations appear, using the examples given in Figure 2a and Figure 2b.

In Figure 2a, the gray state space of a system with two integer state variables is represented. States are represented as dots, polyhedron  $s_1$  contains three states, polyhedra  $s_3$  and  $s_5$  only contain one state *etc.*

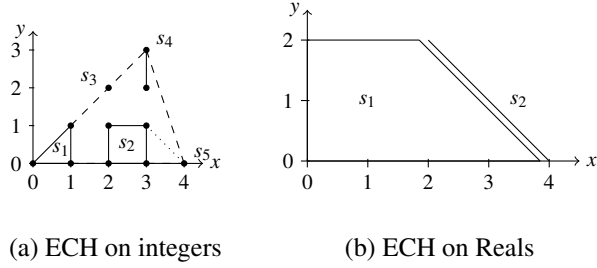


Figure 2: New relations with hulls

Computing exact convex hulls over these base polyhedra in the LIA fragment yields (at least) two new borders, *i.e.* potential relational invariants, pictured as dashed lines. An example of merging order is to merge  $s_1$  with  $s_2$ ,  $s_3$  with  $s_4$ ,  $\{s_1, s_2\}$  with  $\{s_3, s_4\}$ , and  $\{s_1, s_2, s_3, s_4\}$  with  $s_5$  (1).

On a system with real valued state variables however, as shown in Figure 2b, the only case in which we will *discover* a new border by computing exact convex hulls is when one is the limit of another, as illustrated on Figure 2b. Here  $s_1$  is made of  $0 \leq x$ ,  $0 \leq y \leq 2$  and  $y + x - 4 < 0$ ;  $s_2$  is made of  $0 \leq y \leq 2$  and  $y + x - 4 = 0$ , so the resulting hull will be  $0 \leq x$ ,  $0 \leq y \leq 2$  and  $y + x - 4 \leq 0$ . The information learned this way has little chance of strengthening the PO.

As will be seen in the next sections, when trying to discover new relations, ECH-based techniques work best for integer valued systems, while ICH can be beneficial for both real or integer valued systems.

## 6.1 A First Example

We consider a simple example called the double counter<sup>3</sup> with two integer state variables  $x$  and  $y$  and three boolean inputs  $a$ ,  $b$  and  $c$ . Variables  $x$  and  $y$  are initialized to 0, and are both incremented by one when  $a$  is true or keep their current value when  $a$  is false. The variable  $x$  is reset if  $b \vee c$  is true, and saturates at  $n_x$ . The variable  $y$  is reset when  $c$  is true and saturates at  $n_y$ , hence  $y$  cannot be reset without resetting  $x$ , and  $n_x > n_y$ . The proof objective is  $x = n_x \Rightarrow y = n_y$ . Here is a possible transition relation for such a system:

$$T(s, s') = \begin{array}{ll} \text{(if } (b \vee c) & \text{then } x' = 0 \text{ else if } (a \wedge x < n_x) \text{ then } x' = x + 1 \text{ else } x' = x) \\ \wedge & \text{(if } (c) \text{ then } y' = 0 \text{ else if } (a \wedge y < n_y) \text{ then } y' = y + 1 \text{ else } y' = y). \end{array}$$

Let us see now how the proposed approach performs on this system when fixing  $n_x = 10$  and  $n_y = 6$  for instance. First, using the abstract interpretation tool presented in [23], bounds on  $x$  and  $y$  are easily discovered:  $0 \leq x \leq n_x = 10$  and  $0 \leq y \leq n_y = 6$ , yet the PO cannot be proved with AI without further manual intervention. So, using these range properties once  $k$ -induction has confirmed them, we start the backward property-directed analysis, which outputs a first preimage:  $x = 9 \wedge 0 \leq y < 5$  (1).

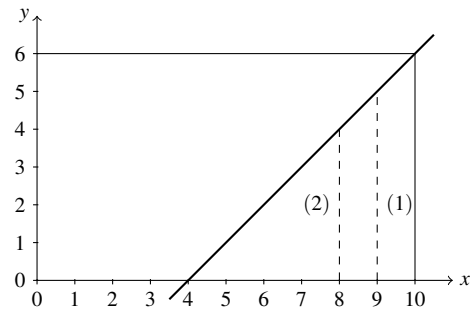


Figure 3: ECH calculation on the double counter

<sup>3</sup>Code available at <http://www.onera.fr/staff-en/adrien-champion/>.



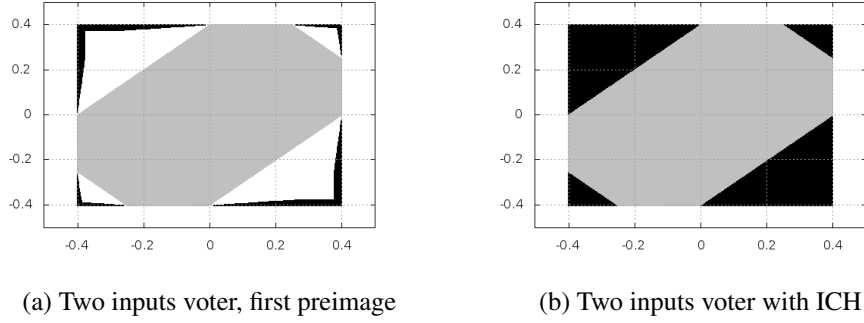


Figure 4: Simple voting logic.

Unsurprisingly, it is too weak to conclude, *i.e.* its negation is not  $k$ -inductive for a small  $k$ . The next preimage is  $x = 8 \wedge 0 \leq y < 4 \vee x = 9 \wedge 0 \leq y < 5$  (2) which does not allow to conclude either for the same reason. Instead of iterating until a fixed point is found, consider the graph on Figure 3. It shows the two first preimages as dashed lines which seem to suggest a relation between  $x$  and  $y$ , pictured as a bold line. This relation can be made explicit by calculating the convex hull of the disjunction of the first two preimages – since this particular system can stutter, it is the same as (2). This yields  $8 \leq x \leq 9 \wedge 0 \leq y < x - 4$ . Note that this convex hull is an ECH, since both  $x$  and  $y$  are integers. The four inequalities are negated – they characterize gray states – and are sent to the  $k$ -induction engine. Potential invariants  $\neg 8 \leq x$ ,  $\neg x \leq 9$  and  $\neg 0 \leq y$  are falsified, and the PO in conjunction with lemma  $\neg y < x - 4$  is found to be 1-inductive.

In fact, this PO could also be proved correct by  $k$ -induction given the bounds found by AI only, by unrolling the transition relation to the recurrence diameter of the system. In practice, even on such a simple system it is not possible for large values of  $n_x$  and  $n_y$  (hundreds or thousands of transitions). The performance of our technique on the other hand is not sensitive to the actual value of numerical constants: it will always derive the strengthening lemma from the first two preimages. Obviously, the time needed to compute the preimages is not impacted by changing the constants values either.

For more complex systems with preimages made of more than two polyhedra, simply merging them in arbitrary order using convex hull calculation is not robust since the resulting convex hulls would depend on the merging order, and interesting polyhedra could be missed. This idea of an exhaustive enumeration of the intermediary ECHs that can appear when merging a set of polyhedra is explored in Section 7.1.

## 6.2 A Second Example

Let us now consider briefly a two input, real valued voting logic system derived from the Rockwell Collins triplex voter. We will not discuss the system itself since the triplex voter is detailed in Section 8.2. It simply allows us to represent graphically the state space in a plan. The PO here is that two of the state variables,  $Equalization_1$  and  $Equalization_2$ , range between  $-0.4$  and  $0.4$ . Figure 4 depicts the corresponding square. On Figure 4a we can see the first preimage calculated by our backward reachability analysis as black triangles, and the strengthening lemmas found by hand in [11] transposed to the two input system as a gray octagon. Calculating ECH on this first preimage does not allow to conclude.

A more relevant approach would be to calculate ICH. Yet, since the ICH of all the preimage polyhedra is the  $[-0.4, 0.4]^2$  square, we need to be more subtle and introduce a criterion for ICH to be actually computed between two polyhedra: they have to intersect. Intersection can be checked by a simple

satisfiability test performed using a SMT solver. This check allows us to identify overlapping areas of the gray state space and to over-approximate them, while not merging disjoint areas in the gray state space explored so far. This approximation obtained through ICH resembles widening techniques used in abstract interpretation [9] in the sense that it allows to *jump* forward in the analysis iterations, yet it differs in the sense that, contrary to widening, it does not ensure termination. The only goal here is to generate potential invariants for the PO, and Figure 4 shows that the ICH yields exactly the dual, in the  $[-0.4, 0.4]^2$  square, of the octagon invariant found by hand in [11]. This second idea of using ICHs to perform overapproximations will be discussed in Section 7.4.

## 7 Generating Potential Lemmas Through Hull Computation

We now detail two heuristics which use the preimages output by the backward analysis. The first one follows the example from Section 6.1 and consists in a thorough, exact exploration of the partitionings of the gray state space. After explaining the basic algorithm in Section 7.1, optimizations are developed in Section 7.2. A small example illustrates the method in Section 7.3. The second heuristic over-approximates areas of the gray state space in the spirit of the discussion in Section 6.2, and is discussed in Section 7.4. Both aim at discovering new relations between the state variables which once negated become potential invariants. Figure 6 provides a high level view of the different components and the way they interact internally and with the exterior.

### 7.1 Hullification Algorithm

The algorithm presented in this section, called *hullification*, calculates all the convex hulls that can be created by iterating the convex hull calculation on a given set of polyhedra, called the *source* polyhedra. In this algorithm we will calculate ECH as opposed to ICH to avoid both losing precision in the process and the potential combinatorial blow up – ICH are used in a different approach in Section 7.4. The difficulty here is to not miss any of the ECH that can be possibly calculated from the source polyhedra. Indeed, back to the example on Figure 2a the merging order (1) misses the ECH of  $s_2$  and  $s_5$  (represented as a dotted line), and consequently the potential relational lemma  $y \leq -x + 4$ , which could have strengthened the PO.

Imperative and slightly object-oriented pseudo-code is provided on Algorithm 1. The purpose of *generatorSetMemory* is related to optimizations, discussed in Section 7.2. Please note that for the sake of clarity, the function called on line 20 is detailed separately on Algorithm 2. The hullification algorithm iterates on a set of pairs called the *generatorSet*: the first component of each of these pairs is a convex hull called the *pivot*. The second one is a set of convex hulls the pivot will be tried to be exactly merged with, called the pivot *seeds*. Note that since the ECHs are calculated by merging polyhedra two by two, our hullification algorithm cannot find convex hulls that require to merge more than two polyhedra at the same time to be exact.

The *generatorSet* is initialized such that for any couple  $(i, j)$  such that  $0 \leq i \leq n$  and  $i < j \leq n$ ,  $p_i$  is a pivot and  $p_j$  is one of its seeds, line 3. A *newgeneratorSet* is initialized with the same pivots as the *generatorSet* but without any seeds (line 8). At each iteration (line 6), a first loop enumerates the pairs of pivot and seeds of the generation set (line 9). Embedded in the first one, a second loop iterates on the seeds (line 11) and tries to calculate the ECH of the pivot and the seed (line 14) as described in Section 4. If the exact merge was successful, the new ECH is added to the seeds of the pivots of the *newGeneratorSet* (line 20, detailed below) and as a new pivot with no seeds. Once the elements of the



**Algorithm 1** Hullification Algorithm:

---

*hullification*( $\{p_i | 0 \leq i \leq n\}$ ).

---

```

1: generatorSetMemory =  $\{\{p_i\} | 0 \leq i \leq n\}$ 
2: sourceMap =  $\{p_i \rightarrow \{p_i\} | 0 \leq i \leq n\}$ 
3: generatorSet =  $\{(p_i, S_i) | 0 \leq i \leq n \wedge S_i = \{p_k | i < k \leq n\}\}$ 
4: generatorSetMemory = generatorSetMemory  $\cup \{\{p_i, p_j\} | 0 \leq i \leq n, i < j \leq n\}$ 
5: fixedPoint = false
6: while ( $\neg$ fixedPoint) do
7:   fixedPoint = true
8:   newGeneratorSet =  $\{(p_i, \{\}) | \exists S, (p_i, S) \in \text{generatorSet}\}$ 
9:   for all  $((\text{pivot}, \text{seeds}) \in \text{generatorSet})$  do
10:    sourcePivot = sourceMap.get(pivot)
11:    for all (seed  $\in$  seeds) do
12:      sourceSeed = sourceMap.get(seed)
13:      source = sourcePivot  $\cup$  sourceSeed
14:      hull = computeHull(pivot, seed)
15:      newGeneratorSet.update(pivot, newGeneratorSet.get(pivot)  $-$  seed)
16:      if (hull  $\neq$  false) then
17:        fixedPoint = false
18:        sourceMap.add(hull  $\rightarrow$  source)
19:        newGeneratorSet =
20:          updateGenSet(hull, source, pivot, seed, newGeneratorSet)
21:      end if
22:    end for
23:  end for
24:  generatorSet = newGeneratorSet
25:  // Communication.
26: end while
27: return  $\{p_i | \exists S, (p_i, S) \in \text{generatorSet}\}$ 

```

---

**Algorithm 2** Updating the *newGeneratorSet*:

---

*updateGenSet*(*hull*, *source*, *newGeneratorSet*).

---

```

1: result =  $\{\}$ 
2: for all  $((\text{pivotAux}, \text{seedsAux}) \in \text{newGeneratorSet})$  do
3:   sourceAux = sourceMap.get(pivotAux)
4:   shallAdd =  $(\text{sourceAux} \cup \text{source}) \notin \text{generatorSetMemory} \ \&\&$ 
5:      $(\text{sourceAux} \not\subseteq \text{source})$ 
6:   if (shallAdd) then
7:     result.update( $(\text{pivotAux}, \text{seedsAux} \cup \{\text{hull}\})$ )
8:     generatorSetMemory.add(sourceAux  $\cup$  source)
9:   else
10:    result.add( $(\text{pivot}, \text{seeds})$ )
11:   end if
12: end for
13: result.add( $(\text{hull}, \{\})$ )
14: return result

```

---

*generatorSet* have all been inspected and if new ECH(s) have been found, a new iteration begins with the *newGeneratorSet*. When no new convex hulls are discovered during an iteration, the algorithm returns all the ECHs found so far (line 27).

## 7.2 Optimizing Hullification

The hullification algorithm is highly combinatorial, and this section presents optimizations that improve its scalability.

In the hullification algorithm, the number of merge attempts increases dramatically depending on the number of elements added in the *generatorSet* at each iteration. With hullification as is, in many cases,

elements of this set can be redundant, in the sense that the new hulls derived from them, if any, would be the same even though the elements are different. The key idea to reducing redundancy is to keep a link between any ECH calculated and the source polyhedra merged to create it, thereafter called the ECH source, and use this information to skip redundant ECH calculation attempts.

Consider for example Figure 5a. If we already tried to merge the ECH of source  $\{s_1, s_2, s_3\}$  with the one of source  $\{s_4, s_5\}$  then it is not necessary to consider trying to merge say the ECH of source  $\{s_3, s_4\}$  with the one of source  $\{s_1, s_2, s_5\}$ . The result would be the same, *i.e.* the same ECH or a failure to merge the convex hulls exactly (the same ECH here). Note that since we are generating all the existing ECHs from the source polyhedra, this case happens every time an ECH can be calculated by merging its source in strictly more than one order, that is to say **very** often. More generally, we do not want to attempt merges of different hulls deriving from the same set of source polyhedra.

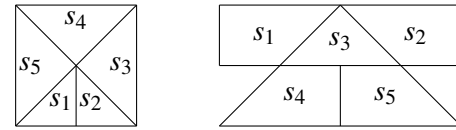
Another source of redundancy is that, when a seed is added to a pivot during the *generatorSet* update, it represents a potential merge of the union of the pivot source and the seed source. Even if this merge has not yet been considered, a potential merge of the same source might have already been added to the *generatorSet* through a different seed added to a different pivot. In this case we do not want the seed to be added. So, in order to prevent redundant elements from being added to the *generatorSet*, we introduce a memory called *generatorSetMemory*, and control how new hulls are added to the *newGeneratorSet*. For a new hull to be added to a pivot as a seed,  $source(pivot) \cup source(hull) \notin generatorSetMemory$  must hold (Algorithm 2 line 4); if the hull is indeed added to the seeds of the pivot, then  $generatorSetMemory += source(pivot) \cup source(hull)$  (Algorithm 2 line 8). Informally, this memory contains the sources of all the potential merges added to the generator set. This ensures that the merge of a source will never be considered more than once, and that the merges we did not consider were not reachable by successive pair-wise ECH calculation.

Also, we forbid adding a seed to a pivot's seeds if the source of the latter is a subset of the former, since the result would necessarily be the seed itself (we call this (1)). Another improvement deals with *when* hullification interacts with the the rest of the framework. Since our goal is to generate potential invariants, we do not need to wait for the hullification algorithm to terminate to communicate the potential invariants already found so far. They are therefore communicated, typically to *k*-induction, after each *big iteration* of the algorithm (loop on Algorithm 1 line 25). This has the added benefit of launching *k*-induction on smaller potential invariant sets.

There is a drawback in comparing hulls using their sources: assume that two of the input (source) polyhedra  $p_i$  and  $p_j$  are such that  $p_i \Rightarrow p_j$ . Then the exact merge of  $p_i$  and  $p_j$  succeeds and yields the hull of source  $\{p_i, p_j\}$ , which is really  $p_j$ . As a consequence, the pivots of the *generatorSet* are redundant, as are their seeds and in the end the merge attempts. To avoid this, we first check the set of input polyhedra and discard redundant ones.

Last but not least, merges are also memorized in between calls to the algorithm so that we do not call the merge algorithm when considering two polyhedra we already merged during a previous call. Since hullification is called on the ever-growing disjunction of all preimages found so far, each new disjunction contains the previous one and this represents a significant improvement.

In the next subsection we illustrate hullification on a small example before introducing another potential invariant generation algorithm in Section 7.4. Hullification will be illustrated on a reconfiguration logic system in Section 8.1



(a) Square example

(b) Hat example

Figure 5: Hullification redundancy issues

### 7.3 Hullification Example

Let us now unroll the algorithm on a simple example depicted on Figure 5b. For the sake of concision a source  $\{s_1, s_2, \dots, s_n\}$  will be written  $12 \dots n$ . We write generator sets in the following fashion:  $\{(pivot, [seeds])\}$ .

With this convention, the initial *generatorSet* is  $\{(1, [2, 3, 4, 5]), (2, [3, 4, 5]), (3, [4, 5]), (4, [5]), (5, [])\}$ . The *newGeneratorSet* for the first *big step* iteration trace is as follows:

1, []	2, []	3, []	4, []	5, []				
1, []	2, [13]	3, []	4, [13]	5, [13]	13, []			
1, []	2, [13]	3, []	4, [13, 23]	5, [13, 23]	13, []	23, []		
1, [45]	2, [13, 45]	3, [45]	4, [13, 23]	5, [13, 23]	13, [45]	23, [45]	45, []	

At first *newGeneratorSet* is the same as *generatorSet* without seeds (first line of the trace). We first consider 1 as a pivot. The merge of 1 and 3 works while the other ones fail, leading to the second line of the trace. Note that 13 is not added to 1 nor 3 since  $1 \subseteq 13$  and  $3 \subseteq 13$  by (1). With this pivot we add three sources to the *generatorSetMemory*: 213, 413 and 513 (2). The next pivot is 2 which is merged with 3 while the merges with the other seeds fail. After the *newGeneratorSet* update we obtain the third line of the trace. Note that 23 is not added to the seeds of 1 since source 213 has already been added to the *generatorSetMemory* at (2) so  $23 \cup 1 \in \text{generatorSetMemory}$ . Similarly, it is not added to the seeds of 13 either. Next pivot 3 cannot be merged with any of its seeds. Pivot 4 can be merged with 5 producing the fourth line of the generator trace. A new big step iteration begins during which 2 will be merged with 13 and 3 with 45 while all the other merges will fail. At the beginning of the third big step iteration the *generatorSet* is

$$\begin{aligned} &\{(1, [345]), (2, [345]), (3, []), (4, [123]), (5, [123]), \\ &(13, [345]), (23, [345]), (45, [123]), (123, [345]), (345, [])\}. \end{aligned}$$

No new hull is found and the algorithm detects that a fixed point has been reached.

### 7.4 Another Way to Generate Potential Invariants: ICHs

As mentioned before in Section 7.1, ECH calculation cannot do much for real state variables. We therefore propose a second approach based on Inexact Convex Hull (ICH) calculation modulo intersection as mentioned in Section 6.2, simply called ICH calculation in the rest of this paper. That is, two polyhedra will be inexactly merged if and only if their intersection is not empty. This regroups areas of the gray state space that are not disjoint and over-approximates them to make new numerical relations appear. An efficient way to check for intersection is to check the satisfiability of the conjunction of the constraints describing the two polyhedra using an SMT solver. Note that this technique is also of interest in the integer case.

For a given set of polyhedra more ICHs than ECHs can be created, in practice often a lot more. The hullification algorithm using ICHs thus tends to choke. We propose the following algorithm, only briefly described for the sake of concision.

Select a pivot in the input polyhedra set and try to find an ICH with the other ones. If an ICH with another polyhedra (source) exists, both the pivot and the source are discarded, and the ICH becomes the new pivot. Once all the merges have been tried, the pivot is put aside and a new pivot is selected in the remaining polyhedra set. When the algorithm runs out of polyhedra, it starts again on the polyhedra put aside if at least one new hull was found. If not, a fixed point has been reached and the algorithm stops.

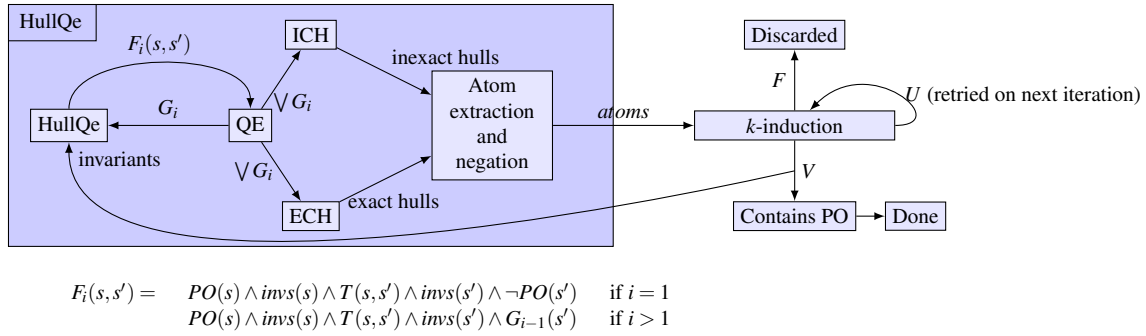


Figure 6: High level sequential description

Although the intermediary ICHs computed in this algorithm depends on the order in which the pivots are selected and merged with the other polyhedra, its result does not. Indeed, the fact that two polyhedra have a non-empty intersection will stay true even if one or both of them are merged with other polyhedra. This result, as depicted in Section 6.2, is an over-approximation of disjoint areas of the gray state space.

In practice, both the ECH based hullification and the ICH calculation heuristics run in parallel, and the sets of potential invariants they output are merged before being sent to the  $k$ -induction. This allows us to combine the precision of ECHs with the over-approximation effect of ICHs. A high level view of our approach is available on Figure 6. The next section will present two examples taken from a functional chain as presented in Section 2 each illustrating the ideas introduced in this section: a reconfiguration logic system and a voting logic system.

## 8 Applications

In this section we discuss the results of the proposed approach on two real world examples: a reconfiguration logic and the triplex voter of Rockwell Collins.

### 8.1 Reconfiguration Logic

Distributed reconfiguration logic as presented in Section 2 would be best described as a distributed priority mechanism. In each redundant channel, the reconfiguration logic comes last and monitors the warning flags raised by the monitoring logic implemented earlier in the data flow. Integer timers and latches are used to confirm warnings over a number of consecutive time steps and trigger a reconfiguration. The duration of the various confirmations can vary from a few steps to hundreds or thousands of steps and are tuned by system designers to be not overly sensitive to transient perturbations, which would unnecessarily trigger reconfigurations of otherwise healthy channels, while being fast enough to ensure safety. Assuming at most two sensors, network or CPU faults, the following generic property is expected to hold for the reconfiguration mechanism: “No unhealthy channel shall be in control for more than  $N$  steps”. This property can be decomposed and instantiated per channel. However, a property such as “No more than one channel shall be in command at any time”, or “The actuator must never stay idle for more than  $m_4$  steps” are more challenging because they cover all three channels simultaneously and drag many state variables in their cone of influence. For instance, the formal verification of the second property is done by assembling a model of the distributed system and by using the synchronous observer technique as shown in Figure 7. The observer uses a timer and is coded so that its output becomes true as soon as

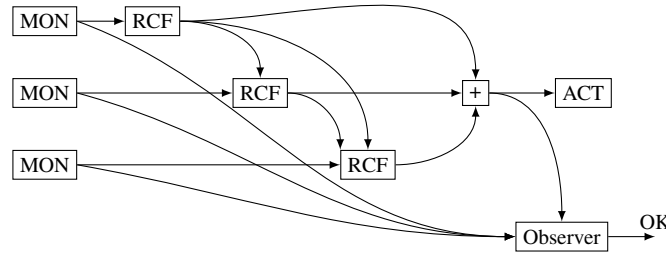


Figure 7: Reconfiguration subsystem with observer.

the absence of control of the actuator has been confirmed for the requested amount of  $m_4$  consecutive steps. The proof objective on the system/observer composition is to show that the output of this observer can never be true.

The timer logic found in this system is similar to that of the toy example developed in Section 6.1, and instantiated several times, indeed a channel becoming corrupt triggers several timers with different bounds, running into each other or in parallel. Let us now see how hullification performs on this system. The first preimage does not contain enough information, since hullification generates no potential lemma which either strengthens the PO or is  $k$ -inductive by itself. The union of the first and second preimages however allows hullification to generate about 200 potential invariants. Once they are negated,  $k$ -induction invalidates most of them and indicates the PO was found (1-)inductive conjoined with about 50 lemmas after about 30 seconds of computation.

After the minimization phase described in Section 6, it turns out that only three lemmas are required. If we call  $timer_i$  the integer variable used to count the time channel  $i$  is not in command for  $1 \leq i \leq 3$ , and  $timer_o$  the timer used by the observer, the lemmas are:  $\neg(timer_o - timer_i \geq m_4 - m_i - 1)$  where  $1 \leq i \leq 3$ . These lemmas are found no matter the values of the  $m_i$  for  $1 \leq i \leq 4$ . We insist on the interest of hullification here. Merging polyhedra in some single arbitrary order is too coarse and the resulting hull cannot strengthen the PO, whereas the thorough exploration generates useful lemmas.

The reconfiguration logic was also analyzed using NBac, Scade Design Verifier and Tinelli's Kind. NBac did not succeed in proving the property after 1 hour of computation. Both the Scade Design Verifier and Kind kept on incrementing the induction depth without finding a proof after 30 minutes of run time.

The invariant generation of Kind was also run on this system, and yielded a number of small theorems, but obviously not property directed and unfortunately not sufficient to strengthen the PO and prove it.

In conclusion, the proposed combination of backward analysis, hullification and  $k$ -induction allows us to complete a proof in a few seconds on a widely used avionics design pattern, where other state of the art tools fail. In addition, we see two very interesting points worth highlighting about hullification: (i) The PO is made (1-)inductive, implying the proof can easily and quickly be re-run and checked by any existing induction tool; (ii) the time needed to complete the proof does not depend on the numerical values of the system –about thirty seconds on a decent machine in practice for this system<sup>4</sup>. This is very important for critical embedded systems manufacturers as point (i) means that the proofs are trustworthy, both for the industrials themselves and the certification organisms. On the other hand, point (ii) implies that strengthening lemmas can be very quickly generated for similar design patterns with altered numerical values, easing the integration of formal verification in the development process. Indeed, it

<sup>4</sup>Using our prototype implementation in Scala.

avoids the need for an expert to manually transpose the lemmas on the new system, as can be the case for complicated and resource/time consuming proofs.

## 8.2 The Triplex Voter

Let us now turn to the Rockwell Collins triplex sensor voter, an industrial example of voting logic as introduced in Section 2, implementing redundancy management for three sensor input values. This voter does not compute an average value, but uses the *middleValue*( $x, y, z$ ) function, which returns the input value, bounded by the minimum and the maximum input values (*i.e.*  $z$  if  $y < z < x$ ). Other voter algorithms which use a (possibly weighted) average value are more sensitive to one of the input values being out of the normal bounds. The values considered for voting are *equalized* by subtracting equalization values from the inputs. The following recursive equations describe the behaviour of the voter with  $X \in \{A, B, C\}$ :

$$\begin{aligned}
 \text{Equalization}X_0 &= 0.0 \\
 \text{Equalized}X_t &= \text{Input}X_t - \text{Equalization}X_t \\
 \text{Equalization}X_{t+1} &= 0.9 * \text{Equalization}X_t + \\
 &\quad 0.05 * (\text{Input}X_t + ((\text{Equalization}X_t - \text{VoterOutput}_t) - \text{Centering}_t)) \\
 \text{Centering}_t &= \text{middleValue}(\text{Equalization}A_t, \text{Equalization}B_t, \\
 &\quad \text{Equalization}C_t) \\
 \text{VoterOutput}_t &= \text{middleValue}(\text{Equalized}A_t, \text{Equalized}B_t, \text{Equalized}C_t)
 \end{aligned}$$

The role of the equalization values is to compensate offset errors of the sensors, assuming that the middle value gives the most accurate measurement.

We are interested in proving Bounded-Input Bounded-Output (BIBO) stability of the voter, which is a fundamental requirement for filtering and signal processing systems, ensuring that the system output cannot grow indefinitely as long as the system input stays within a certain range. In general, it is necessary to identify and prove auxiliary system invariants in order to prove BIBO stability.

So, we want to prove the stability of the system, *i.e.* we want to prove that the voter output is bounded as long as the input values differ by at most the maximal authorized deviation *MaxDev* from the true value of the measured physical quantity represented by the variable *TrueValue*. In our analysis, we fixed the maximal sensor deviation to 0.2, a value that domain experts gave us as typical value in practical applications. It is straightforward to prove that the system is stable if the equalization values are bounded.

When applied to Rockwell Collins **triplex** sensor voter, our prototype implementation manages to prove the PO in less than 10 seconds by discovering that  $-0.9 \leq \sum_{i=1}^3 \text{Equalization}_i \leq 0.9$  is a strengthening lemma, using ICH calculation. Again, the time taken to complete the proof does not depend on the system numerical constants, and the strengthened PO is (1-)inductive. We insist on the importance of these characteristics for both industrials and certification organisms: the proof is trustworthy and can be redone easily for similar, slightly altered designs.

The stability of the system without fault detection nor reset was already proven in [11], but the necessary lemmas had to be found by hand after the Scade Design Verifier, Kind as well as Astrée (which was run on C-Code generated from the Lustre source) failed at automatically verifying the BIBO property.



## 9 Framework and Implementation

Our actor oriented collaborative verification framework [8] called *Stuff* is composed of several elements: the  $k$ -induction engine, the abstract interpreter, the backward analysis, ICH calculation and ECH hullification. They can all evolve in parallel and communicate.

*Stuff* is written in Scala except for the abstract interpreter, written in OCaml. We implemented the backward analysis and the two heuristics presented in this paper using the QE algorithm from [19] modified to handle integers or reals with booleans. The underlying projections of [19] are performed by the Parma Polyhedra Library [1], also used for convex hull computation. *Stuff* can use any SMT lib 2.0 [2] compliant solver thanks to the Assumptio<sup>5</sup> actor oriented SMT solver wrapper. In practice, the backward analysis and the heuristics use Microsoft Research Z3 [20] and MathSat 5 [14] by the University of Trento.

A run of the framework in the default configuration begins by a preprocessing phase using abstract interpretation with intervals as abstract domains in order to infer bounds on the state variables. This provides an over-approximation of the reachable state space which once verified by  $k$ -induction is propagated to all the other elements of the framework. The rest of the analysis follows the approach discussed in Section 6 with the backward analysis feeding preimages to both ECH hullification and ICH calculation. They in turn feed potential invariants to the  $k$ -induction engine which detects real invariants and check if they strengthen the property as described in Section 6. In this setting, even if our approach does not consider the initial states, it benefits from the over-approximation of the AI preprocessing phase, which takes into account the initial states but not the PO. The AI results also enhance the quality of the output and the overall performance of the incremental  $k$ -induction engine.

## 10 Conclusion

In this paper, the authors presented two automatic and property directed lemma generation heuristics, which operate on preimages of the negation of the proof objective obtained by a backward exploration, itself powered by quantifier elimination.

The first heuristic originality lies in the thorough exploration of a set of possible convex partitionings of the gray state space by exact convex hull calculations. This exploration, called *hullification*, is performed incrementally, as soon as new preimages containing new information about the gray state space, are computed by the backward analysis. As illustrated on the reconfiguration logic example, the blowup inherent to the exploration of the partitionings is avoided thanks to the optimizations discussed in this paper and far outperforms other available tools.

The second heuristic over-approximates disjoint areas of the gray state space by accepting inexact hulls when the candidate polyhedra intersect. It performs very well in the Rockwell Collins Triplex Sensor Voter experiments, allowing to conclude a proof none of the other state of the art tools could conclude.

These results, obtained with the prototype implementation of the proposed method, are of interest in our application field. Indeed, they allow to discover strengthening lemmas, in reasonable time, for essential safety properties of widely used fault tolerance design patterns at model level, a task which has proved difficult to achieve using other techniques such as AI or  $k$ -induction with manual analysis of failed proofs.

---

<sup>5</sup><https://cavale.enseeiht.fr/redmine/projects/assumptio>

Future work include further reflexion on systems mixing integers and reals and on heuristics using preimages from the backward analysis. Also, the authors think that when hullification cannot find strengthening lemmas, it can still provide interesting starting points for template based techniques and experiments have been started in this direction. Outside of the proposed approach, the authors believe in a multi method approach and will continue to experiment in this direction: work on an implementation of PDR [5, 13] adapted to numerical systems is in progress. It was observed that PDR is able to discover range lemmas similar to those found using interval based AI, while being able to conclude inductive proofs, and the cooperation of hullification and PDR is being studied. The long term goal is to refine and bridge the verification techniques developed for precise parts of the functional chains (voting, reconfiguration logic and numerical stability for control laws) to obtain a methodology and tool support suitable for end-to-end verification of avionics software at model level.

## References

- [1] R. Bagnara, P. M. Hill & E. Zaffanella (2008): *The Parma Polyhedra Library: Toward a Complete Set of Numerical Abstractions for the Analysis and Verification of Hardware and Software Systems*. *Science of Computer Programming* 72(1–2), pp. 3–21. Available at <http://doi.acm.org/10.1016/j.scico.2007.08.001>.
- [2] C. Barrett, A. Stump, C. Tinelli, S. Boehme, D. Cok, D. Deharbe, B. Dutertre, P. Fontaine, V. Ganesh, A. Griggio, J. Grundy, P. Jackson, A. Oliveras, S. Krstić, M. Moskal, L. de Moura, R. Sebastiani, T. D. Cok & J. Hoenicke (2010): *C.: The SMT-LIB Standard: Version 2.0*. Available at <http://citeseerx.ist.psu.edu/viewdoc/summary?doi=10.1.1.190.4897>.
- [3] N. Bjørner (2010): *Linear Quantifier Elimination as an Abstract Decision Procedure*. In Jürgen Giesl & Reiner Hahnle, editors: *Automated Reasoning, Lecture Notes in Computer Science* 6173, Springer Berlin / Heidelberg, pp. 316–330. Available at [http://dx.doi.org/10.1007/978-3-642-14203-1\\_27](http://dx.doi.org/10.1007/978-3-642-14203-1_27).
- [4] B. Blanchet, P. Cousot, R. Cousot, J. Feret, L. Mauborgne, A. Miné, D. Monniaux & X. Rival (2003): *A Static Analyzer for Large Safety-Critical Software*. In: *Proceedings of the ACM SIGPLAN 2003 Conference on Programming Language Design and Implementation (PLDI'03)*, ACM Press, San Diego, California, USA, pp. 196–207. Available at <http://dx.doi.org/10.1145/781131.781153>.
- [5] A. R. Bradley (2011): *SAT-Based Model Checking without Unrolling*. In: *VMCAI*, pp. 70–87. Available at [http://dx.doi.org/10.1007/978-3-642-18275-4\\_7](http://dx.doi.org/10.1007/978-3-642-18275-4_7).
- [6] A. R. Bradley & Z. Manna (2006): *Verification Constraint Problems with Strengthening*. In: *ICTAC*, pp. 35–49. Available at [http://dx.doi.org/10.1007/11921240\\_3](http://dx.doi.org/10.1007/11921240_3).
- [7] P. Caspi, D. Pilaud, N. Halbwachs & J. Plaice (1987): *Lustre: A Declarative Language for Programming Synchronous Systems*. In: *POPL*, pp. 178–188. Available at <http://doi.acm.org/10.1145/41625.41641>.
- [8] A. Champion, R. Delmas, P.L. Garoche & P. Roux (2011): *Towards Cooperation of Formal Methods for the Analysis of Critical Control Systems*. In: *SAE Int. J. Aeroesp.*, pp. 850–858. Available at <http://dx.doi.org/10.4271/2011-01-2558>.
- [9] P. Cousot & R. Cousot (1977): *Abstract Interpretation: A Unified Lattice Model for Static Analysis of Programs by Construction or Approximation of Fixpoints*. In: *POPL*, pp. 238–252. Available at <http://doi.acm.org/10.1145/512950.512973>.
- [10] Werner Damm, Stefan Disch, Hardi Hungar, Swen Jacobs, Jun Pang, Florian Pigorsch, Christoph Scholl, Uwe Waldmann & Boris Wirtz (2007): *Exact State Set Representations in the Verification of Linear Hybrid Systems with Large Discrete State Space*. In: *ATVA*, pp. 425–440. Available at [http://dx.doi.org/10.1007/978-3-540-75596-8\\_30](http://dx.doi.org/10.1007/978-3-540-75596-8_30).

- [11] M. Dierkes (2011): *Formal Analysis of a Triplex Sensor Voter in an Industrial Context*. In G. Salaün & B. Schätz, editors: *Proceedings of the 16th edition of FMICS*, LNCS 6959, Springer, pp. 102–116. Available at [http://dx.doi.org/10.1007/978-3-642-24431-5\\_9](http://dx.doi.org/10.1007/978-3-642-24431-5_9).
- [12] M. Dierkes & D. Kästner (2012): *Transferring Stability Proof Obligations from Model Level to Code Level*. Available at <http://www.erts2012.org/Site/OP2RUC89/5C-1.pdf>.
- [13] N. Een, A. Mishchenko & R. Brayton (2011): *Efficient Implementation of Property Directed Reachability*. Available at <http://dl.acm.org/citation.cfm?id=2157675>.
- [14] A. Griggio (2012): *A Practical Approach to Satisfiability Modulo Linear Integer Arithmetic*. JSAT 8, pp. 1–27. Available at [http://jsat.ewi.tudelft.nl/content/volume8/JSAT8\\_1-Griggio.pdf](http://jsat.ewi.tudelft.nl/content/volume8/JSAT8_1-Griggio.pdf).
- [15] B. Jeannet (2003): *Dynamic Partitioning in Linear Relation Analysis: Application to the Verification of Reactive Systems*. *Formal Methods in System Design* 23(1), pp. 5–37. Available at <http://dx.doi.org/10.1023/A:1024480913162>.
- [16] T. Kahsai, Y. Ge & C. Tinelli (2011): *Instantiation-Based Invariant Discovery*. In M. Bobaru, K. Havelund & G. Holzmann & R. Joshi, editors: *Proceedings of the 3rd NASA Formal Methods Symposium (Pasadena, CA, USA)*, Lecture Notes in Computer Science 6617, Springer, pp. 192–207. Available at <http://dl.acm.org/citation.cfm?id=1986326>.
- [17] T. Kahsai & C. Tinelli (2011): *PKind: A parallel k-induction based model checker*. In: *PDMC*, pp. 55–62. Available at <http://dx.doi.org/10.4204/EPTCS.72.6>.
- [18] Kenneth L. McMillan (2008): *Quantified Invariant Generation Using an Interpolating Saturation Prover*. In: *TACAS*, pp. 413–427. Available at [http://dx.doi.org/10.1007/978-3-540-78800-3\\_31](http://dx.doi.org/10.1007/978-3-540-78800-3_31).
- [19] D. Monniaux (2008): *A Quantifier Elimination Algorithm for Linear Real Arithmetic*. In: *LPAR*, pp. 243–257. Available at [http://dx.doi.org/10.1007/978-3-540-89439-1\\_18](http://dx.doi.org/10.1007/978-3-540-89439-1_18).
- [20] L. M. de Moura & N. Bjørner (2008): *Z3: An Efficient SMT Solver*. In: *TACAS*, pp. 337–340. Available at [http://dx.doi.org/10.1007/978-3-540-78800-3\\_24](http://dx.doi.org/10.1007/978-3-540-78800-3_24).
- [21] L. M. de Moura, H. Rueß & M. Sorea (2003): *Bounded Model Checking and Induction: From Refutation to Verification (Extended Abstract, Category A)*. In: *CAV*, pp. 14–26. Available at [http://doi.acm.org/10.1007/978-3-540-45069-6\\_2](http://doi.acm.org/10.1007/978-3-540-45069-6_2).
- [22] T. Nipkow (2010): *Linear Quantifier Elimination*. *J. Autom. Reasoning* 45(2), pp. 189–212. Available at <http://dx.doi.org/10.1007/s10817-010-9183-0>.
- [23] P. Roux, R. Delmas & P.L. Garoche (2010): *SMT-AI: an Abstract Interpreter as Oracle for k-induction*. *Electr. Notes Theor. Comput. Sci.* 267(2). Available at <http://dx.doi.org/10.1016/j.entcs.2010.09.018>.
- [24] P. Roux, R. Jobredeaux, P.L. Garoche & E. Féron (2012): *A generic ellipsoid abstract domain for linear time invariant systems*. In: *Proceedings of the 15th ACM international conference on Hybrid Systems: Computation and Control*, pp. 105–114. Available at <http://doi.acm.org/10.1145/2185632.2185651>.
- [25] M. Sheeran, S. Singh & G. Stålmarck (2000): *Checking Safety Properties Using Induction and a SAT-Solver*. In: *FMCAD*, pp. 108–125. Available at [http://dx.doi.org/10.1007/3-540-40922-X\\_8](http://dx.doi.org/10.1007/3-540-40922-X_8).